symmetry

MDPI

Article

Implementing a Relativistic Motor over Atomic Scales

Asher Yahalom [1,2]

[1] Department of Electrical & Electronic Engineering, Faculty of Engineering, Ariel University, Ariel 40700, Israel; asya@ariel.ac.il; Tel.: +972-54-7740294
[2] Center for Astrophysics, Geophysics, and Space Sciences (AGASS), Ariel University, Ariel 40700, Israel

Abstract: A relativistic motor exchanging momentum and energy with an electromagnetic field is studied. We discuss the advantages and challenges of this novel mover, giving specific emphasis to the more favorable (yet challenging) nano configurations. It specifically turns out that an **isolated** hydrogen atom in either a ground or excited state does not produce relativistic motor momentum.

Keywords: relativity; nanotechnology; relativistic engine

check for updates

Citation: Yahalom, A. Implementing a Relativistic Motor over Atomic Scales. *Symmetry* **2023**, *15*, 1613. https://doi.org/10.3390/sym15081613

Academic Editor: Yiming Huo

Received: 13 July 2023
Revised: 16 August 2023
Accepted: 18 August 2023
Published: 21 August 2023

1. Introduction

Linear momentum is not only a property of matter but also a property of the electromagnetic field [1–3]. Thus, in principle, a vehicle might propagate using the energy supplied by the sun and contained within its storage devices, while the momentum it gains is balanced by the same amount of momentum but of opposite direction, which is transferred to the electromagnetic field.

A detailed introduction to the subject of relativistic motors in general and microscopic relativistic engines in particular with suitable references can be found in [4] and will not be repeated here; the interested reader is referred to the original text. A brief history of the relativistic engine is given below.

The first relativistic engine suggested was based on the electromagnetic field retardation of two time-dependent loop currents [5] (see Figure 1).

Figure 1. Two current loops.

Griffiths and Heald [6] pointed out that strictly Coulomb's law and the Biot–Savart law determine the electric and magnetic fields for static sources only. Thus, Jefimenko's [7] formula was used to calculate the total force $\vec{F}_T$ operating on the center of mass of a system (Jefimenko's equation can also be found in Jackson's book [3]), resulting in the formula

$$\vec{F}_T \cong \frac{\mu_0}{8\pi}(\frac{h}{c})^2\vec{K}_{122}I_2I_1^{(2)}(t), \qquad I_1^{(n)}(t) \equiv \frac{\partial^n I_1(t)}{\partial t^n} \tag{1}$$

in which μ_0 is the magnetic permeability of the vacuum, c is the velocity of light in the vacuum, h is at a typical length scale of the system, and $\vec{K}_{122}$ is a dimensionless vector that depends on the geometry of the loops. I_2 is a static current, and $I_1(t)$ is a time-dependent current. This was later generalized to calculate the total force in a system of a permanent magnet and a current loop [8]. As force is applied for a finite duration, momentum will be acquired, as well as kinetic energy for the entire system. It may superficially seem that the laws of momentum and energy conservation are violated, but this is not so. Linear momentum conservation was validated in [1]. It was shown that the momentum gained by the field $\vec{P}_{field\ 12}$ is the same as the momentum gained by the engine $\vec{P}_{mech}$ but in an opposite direction:

$$\vec{P}_{field\ 12} = -\frac{\mu_0}{8\pi} I_2 I_1^{(1)}(t) \frac{h^2}{c^2} \vec{K}_{122} = -\vec{P}_{mech}. \tag{2}$$

We assumed that the magnetization and polarization of the medium are small and, therefore, neglected corrections to the Lorentz force suggested in [9]. The exchange of energy between the kinetic part of the relativistic engine and the electromagnetic field was elaborated in [10]. It was demonstrated that the electromagnetic energy consumed is six times the engine's kinetic energy. It was also demonstrated that energy is radiated if the coils are misaligned.

Our preliminary analysis assumed bodies that were electric charge natural. In a later paper [11], charged bodies were analyzed. The charged engine allows having a finite momentum even if the current does not increase continuously, as is dictated by the current derivative term in Equation (2) (which requires a monotonously increasing current for a uniform motion in some direction). This more general case result is a total force in the center of mass and total linear momentum given by the formulae

$$\vec{F}_T = \frac{\mu_0}{4\pi} \partial_t \int \int d^3x_1 d^3x_2 \left[\frac{1}{2} (\rho_2 \partial_t \rho_1 - \rho_1 \partial_t \rho_2) \hat{R} - (\rho_1 \vec{J}_2 + \rho_2 \vec{J}_1) R^{-1} \right], \ \vec{R} \equiv \vec{x}_1 - \vec{x}_2 \tag{3}$$

$$\vec{P}_{mech}(t) = \frac{\mu_0}{4\pi} \int \int d^3x_1 d^3x_2 \left[\frac{1}{2} (\rho_2 \partial_t \rho_1 - \rho_1 \partial_t \rho_2) \hat{R} - (\rho_1 \vec{J}_2 + \rho_2 \vec{J}_1) R^{-1} \right] \tag{4}$$

in the above ρ is the charge density and $\vec{J}$ is the current density of the two subsystems 1 and 2, respectively, and an integrations is required over the volumes of the two sub systems. The above equation is valid for both a system containing just two point particles (or a few point particles) in which the charge densities are described by Dirac delta functions, and also in the case of macroscopic number of point particles in which the charge densities can be described by smooth functions.

However, due to dielectric breakdown that dictated a maximal value to charge density [12–15] and current density limitations [16] that limit the amount of current that can be transferred even through a superconducting wire, it is shown that for any reasonable geometrical size, the momentum that can be gained by a relativistic charged engine is very limited. Table 1, obtained from [11], demonstrates the severe limitations of macroscopic configurations:

Table 1. Maximal momentum of a relativistic motor for three cases. We assume an extreme charge density, $\sigma = 3.7 \times 10^{-3}$ Coulomb/m^2, and current density, $J_0 = 5 \times 10^7$ Ampere/m^2.

	Car	**Rocket Size Engine**	**Giant Cube**	**Units**
a	6	200	1000	m
b	2	10	1000	m
d	1	10	1000	m
w	0.2	0.4	0.4	m
P_{mech}	0.3	868	3.1×10^7	kg m/s

The physical structure of this particular relativistic engine and its geometric parameters are depicted in Figures 2 and 3.

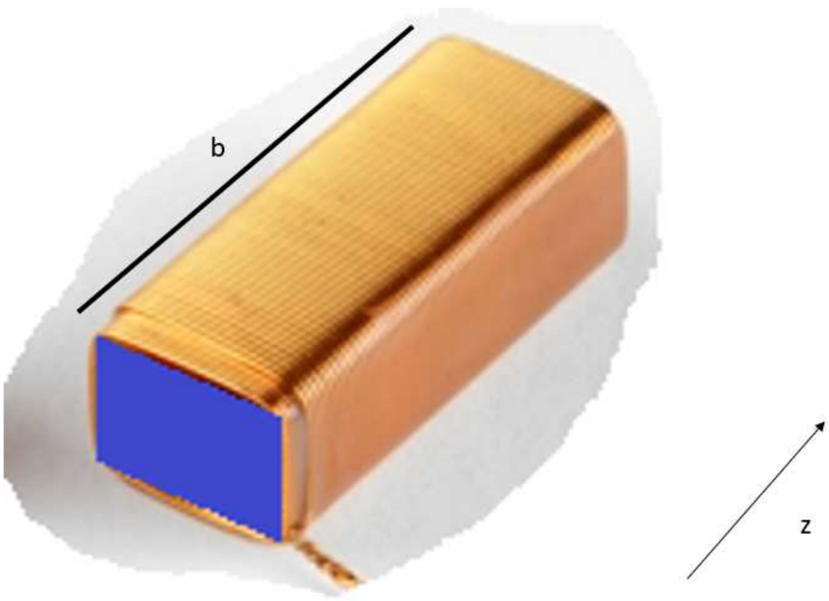

Figure 2. A relativistic engine.

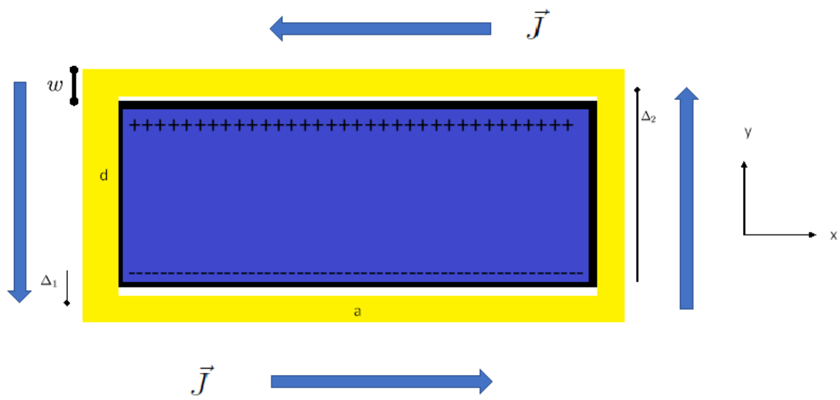

Figure 3. A cross section of the relativistic engine.

The above limitations suggested the use of the high charge densities that are available on the microscopic scale, for example, in ionic crystals. We have pursued this idea in a previous paper [4] in which we calculated the extremely high charge densities and current densities on the atomic scale. It was shown [4] that an **isolated** hydrogen atom in either a ground or excited state does not produce relativistic motor momentum. This is not the case when the atom interacts with other atoms or particles, or when the atom's electron is in a state that is not an eigenstate. Thus, we suggested two naive forms for a wave function in terms of beneficial relativistic engine gain: a wave packet in a hydrogen atom and an eigenstate in a simple molecule, which introduces a static electric field of a broken spherical symmetry.

To conclude, the relativistic motor possesses the following attributes:

- Allows three-axis motion (including vertical);
- No moving parts;
- Zero fuel consumption;
- Zero carbon emission;
- Needs only electromagnetic energy (which may be provided by solar panels);
- Highly efficient, in principle, kinetic energy can be converted back to electromagnetic energy.

However, to reach a practical relativistic engine, one must manipulate matter at subatomic levels, a feat that is quite challenging. In this paper, we shall investigate two ways of doing so, one that is related to free electrons and the other to confined electrons. While we start with a classical description of the problem, we cannot and do not ignore the fact that, on the atomic level, a quantum description is required. It will be shown that the quantum effects are much more important for confined electrons than for free electrons. We shall not derive the equations of the relativistic motor here; the reader is referred to [4,11]. We shall also use the same notations as in the previous papers and will not redefine the symbols.

In the current paper, we will show that both free electrons and confined electrons can be put in a configuration supporting a relativistic motor effect. However, quantum mechanics (for spin and spinless electrons) is only important in the confined electron case. We thus derive the form of the electromagnetic field needed to maintain the appropriate wave packet that supports a relativistic engine effect in the confined case.

2. Relativistic Engine in the Microscopic Scale

2.1. A Classical Electron

Before introducing quantum considerations, we shall first consider a classical system of two point particles each with a charge of absolute value $|e|$. We shall assume one charge to be stationary while the other moving with velocity $\vec{v}_2$; it thus follows that system 2 has a current density of [11]

$$\vec{J}_2 = \rho_2 \vec{v}_2 = e\delta^3(\vec{x}_2 - \vec{x}(t))\vec{v}_2 \tag{5}$$

and system 1 has a charge density of

$$\rho_1 = \pm e\delta^3(\vec{x}_1), \tag{6}$$

in which we assume for convenience that the stationary charge is located at the origin of the coordinates.

2.1.1. Proximity Considerations

Plugging Equations (5) and (6) into Equation (3) of [4]:

$$\vec{P}(t) = -\frac{\mu_0}{4\pi}\int\int d^3x_1 d^3x_2\, \rho_1 \vec{J}_2 R^{-1} = \mp\frac{\mu_0 e^2}{4\pi}\frac{\vec{v}_2}{|\vec{x}(t)|} \tag{7}$$

Taking the total mass of the two particle systems to be $m_t = m_1 + m_2$, we arrive at a center of mass velocity:

$$\vec{v}_{cm}(t) = \frac{\vec{P}(t)}{m_t} = \mp\frac{\mu_0 e^2}{4\pi m_t}\frac{\vec{v}_2}{|\vec{x}(t)|}. \tag{8}$$

The above equation makes explicit the fundamental conflicting requirements of the concept. To have significant speed in the center of mass, the particles must be close to each other; thus, we would like to have a confined system. On the other hand, we would like to have a high v_2 with a constant direction; this is impossible in a confined system as in such a case, $\vec{v}_2$ must eventually change direction. Thus, for the center of mass to obtain speed $v_{cm}(t)$ at time t, the particles must be at the proximity:

$$|\vec{x}(t)| = \mp\frac{\mu_0 e^2}{4\pi m_t}\frac{v_2}{v_{cm}(t)}. \tag{9}$$

If the particles are an electron and a proton $m_t \simeq m_p$,

$$|\vec{x}(t)| = \frac{\mu_0 e^2}{4\pi m_p}\frac{v_2}{v_{cm}(t)}. \tag{10}$$

It is not difficult to bring an electron to move very close to the speed of light such that $v_2 \simeq c$, for example, for 99% of the speed of light with a low-energy accelerator:

$$v_2 = 0.99c \quad \Rightarrow \quad E_k = \frac{m_e c^2}{\sqrt{1 - (\frac{v_2}{c})^2}} \simeq 3.6\,\text{MeV}. \tag{11}$$

Thus, we shall take $v_2 = c$ and obtain

$$|\vec{x}(t)| = \frac{\mu_0 e^2 c}{4\pi m_p} \frac{1}{v_{cm}(t)} = \frac{4.6 \times 10^{-10}}{v_{cm}(t)} = 8.7 \frac{a_0}{v_{cm}(t)}, \tag{12}$$

in which the last expression contains the Bohr radius:

$$a_0 \equiv \frac{4\pi\epsilon_0 \hbar^2}{m'_e e^2} \simeq \frac{\hbar^2}{k m_e e^2} \simeq 0.53 \times 10^{-10}\ \text{m}\,, \qquad m'_e \equiv \frac{m_e m_p}{m_e + m_p} \simeq m_e. \tag{13}$$

The relation between the required distance and the desired velocity for the two particle systems is described in Figure 4.

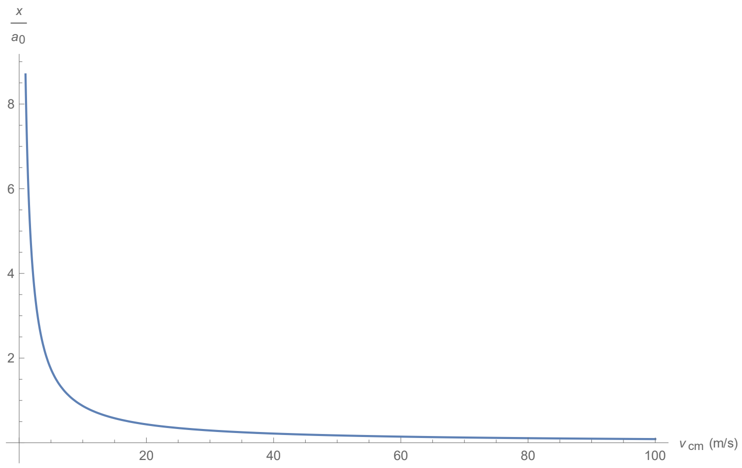

Figure 4. The proximity between a classical electron and proton needed to achieve a desired velocity for an unloaded engine.

Thus, a typical car's velocity, $v_{cm} = 50\ \text{m/s} = 180\ \text{km/h}$, is obtained for

$$|\vec{x}(t)| \simeq 0.174\, a_0. \tag{14}$$

Requiring the hydrogen relativistic motor to escape the earth's gravity (escape velocity of $v_{cm} = 11.2\ \text{km/s}$), we must have a proximity of

$$|\vec{x}(t)| \simeq 48.8\, r_p \tag{15}$$

where $r_p \equiv 8.4 \times 10^{-16}$ m is the proton charge radius. Thus, the distance between electron and proton must be of a nuclear scale rather than an atomic scale. Finally, if we imagine that the relativistic engine can reach relativistic velocities $v_{cm} \simeq 0.1c$, it follows that

$$|\vec{x}(t)| \simeq 0.018\, r_p \tag{16}$$

That is, the electron proton system is of subnuclear dimensions.

An engine suitable for interplanetary travel must include a macroscopic amount of such atoms, and it must carry not just itself but also some payload.

2.1.2. An Unconfined Electron

It seems that a way to circumvent this inherent contradiction between proximity and velocity is to use a train of particles in which for each particle leaving the desired range, a new one enters, as depicted in Figure 5.

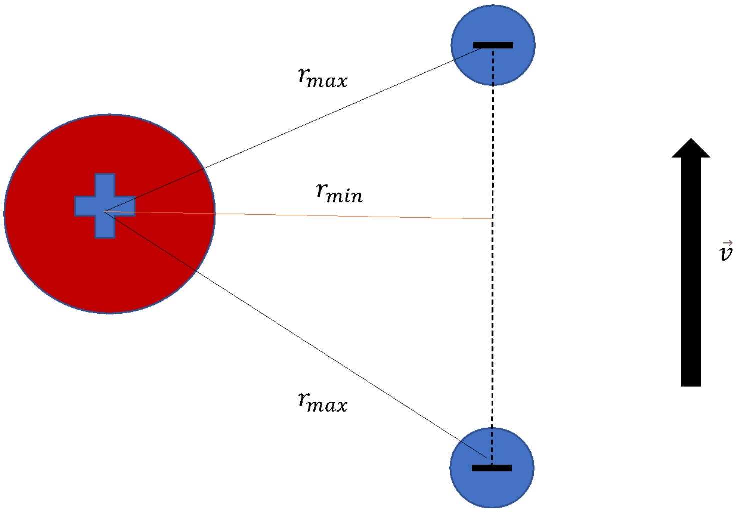

Figure 5. Two electrons from a train of electrons, moving in the vicinity of a proton.

Let us assume that we keep at least one electron from the proton at a distance that is not smaller than a distance r_{max} and bigger that a distance r_{min}; it follows that the duration between successive electrons is

$$\Delta t = 2\frac{\sqrt{r_{max}^2 - r_{min}^2}}{c} \tag{17}$$

If we take r_{min} to be the distance for $v_{cm} = 50$ m/s, that is, $r_{min} = 0.174\, a_0$ and $r_{max} = 3r_{min}$, it follows that

$$\Delta t \simeq 1.7 \times 10^{-19}\text{s} \quad \Rightarrow \quad I = \frac{e}{\Delta t} \simeq 0.92 \text{ A} \tag{18}$$

Hence, the needed current is not too excessive. The practical problem is how to put high-velocity electrons in the vicinity of protons. One may imagine a high-density plasma (see Figure 6)

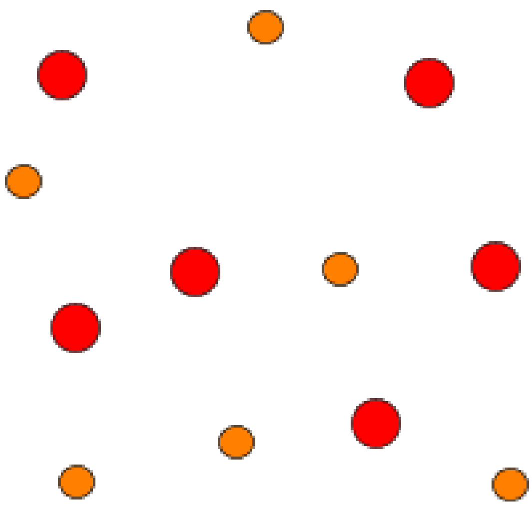

Figure 6. Plasma of protons and electrons: the red circles symbolize protons, while the orange circles symbolize electrons.

made of protons and electrons in which the average density between protons is $2r_{min}$, and the density of such a plasma is

$$\Delta V = (2r_{min})^3 \simeq 6.2 \times 10^{-33}\ \mathrm{m}^3 \quad \Rightarrow \quad \rho_{plasma} = \frac{m_p}{\Delta V} \simeq 2.7 \times 10^5\ \mathrm{Kg/m}^3 \tag{19}$$

This is much higher than the density of solid hydrogen $rho_{SH} \simeq 86\ \mathrm{Kg/m}^3$, in which the typical distance between atoms is about 5 Bohr radii. We notice that a 3.7 L of the above plasma will weigh about 1 metric ton, and could easily move a standard car. We also notice that solid hydrogen can only be obtained under unusual conditions of low temperature and high pressure. Another alternative is to have sparse protons but high-density electrons with a typical distance of $2r_{min}$. However, this will lead ΔV of Equation (19) to a charge density of

$$\rho_{charge} = \frac{e}{\Delta V} \simeq 2.6 \times 10^{13}\ \mathrm{C/m}^3 \tag{20}$$

Obviously, such a configuration cannot hold. If we take for simplicity the configuration to be spherical of radius r_s, then according to Equation (9) of [4], the electric field on its surface would be

$$E_r = \frac{kQ}{r_s^2} = \frac{k\frac{4\pi}{3}\rho_{charge} r_s^3}{r_s^2} = k\frac{4\pi}{3}\rho_{charge} r_s \simeq 9.7 \times 10^{23} r_s \tag{21}$$

Thus, an electron on the surface of the said sphere will be accelerated outwards with an acceleration of

$$\ddot{r} = \frac{eE_r}{m_e} \simeq 1.7 \times 10^{35} r_s\ \mathrm{m/s}^2. \tag{22}$$

The typical disintegration time of the above configuration is

$$\tau_{disintegration} = \sqrt{\frac{r_s}{\ddot{r}}} \simeq 2.4 \times 10^{-18}\ \mathrm{s}, \tag{23}$$

regardless of the size of the sphere. We shall make a point regarding the typical charge separation that is empirically available. According to Section 6, the maximal charge density for air is $\sigma_{max} \simeq 53\ \mu\mathrm{C\ /m}^2$. In terms of electron number density, this is

$$\sigma_{max\ electrons} = \frac{\sigma_{max}}{|e|} \simeq 3.3 \times 10^{14}\ \mathrm{m}^{-2} \tag{24}$$

which translates into a typical spatial separation of

$$\delta_e = \frac{1}{\sqrt{\sigma_{max\ electrons}}} \simeq 5.5 \times 10^{-8}\ \mathrm{m} \tag{25}$$

This separation is much too large to obtain a significant relativistic motor effect. On the other hand, looking back at the ionic crystal of Figure 1 of [4], it is easy to draw a trajectory for the said stream of electrons, as depicted in Figure 7.

As the electron passes through more positive ions, it becomes closer to the positive ion; in fact, even an electron at a distance of a lattice constant of $l \simeq 564$ pm will feel a force perpendicular to its trajectory and towards the positive ion line of about

$$F_\perp \simeq \frac{ke^2}{l} \simeq 4 \times 10^{-19}\ \text{Newton}. \tag{26}$$

Thus, it will have a perpendicular acceleration towards a positive ion line of about

$$\ddot{r}_\perp = \frac{F_\perp}{m_e} \simeq 4.5 \times 10^{11}\ \mathrm{m/s}^2, \tag{27}$$

for a duration of about Δt (see Equation (18)) in each ion passage. Thus, the velocity towards the positive ion line would be at least

$$v_\perp \simeq \Delta t \ddot{r}_\perp \simeq 7.8 \times 10^{-8} \text{ m/s}, \tag{28}$$

but of course, the acceleration and velocity will become larger as the electron reaches closer to the ion line. Thus, the electron will reach the ion line at a time shorter than

$$\tau_{ion\ line} \simeq \frac{v_\perp}{l} \simeq 0.007 \text{ s}. \tag{29}$$

This time can be shortened by applying an external electric field perpendicular to the ion line and away from the line. Moreover, a slower electron beam will have more time to converge to the ion line, which poses an interesting optimization problem, balancing between the desired proximity to the ion line and the electron beam speed. We notice that a 99% speed of light will hardly converge to the ion line even if the engine is 1 meter thick, because it will pass it in about 3 nanoseconds. If convergence to the ion line is indeed achieved, we expect an oscillatory motion around the positive ion line in which inverse beta decay will occasionally occur. Of course, the most significant relativistic motor effects will occur at the times in which the electron is closer to the positive ion line.

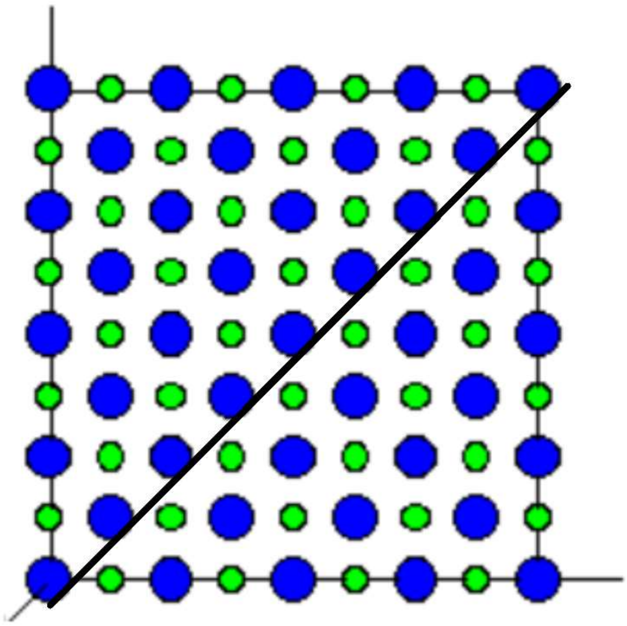

Figure 7. The 100 planes of a lattice of Na^+Cl^- (table salt): blue circles depict sodium positive ions, and green circles depict chlorine negative ions. The trajectory of relativistic electrons is described using a thick black line.

2.1.3. A Confined Electron

A confined classical electron can be put in an elliptical trajectory that can be occasionally favorable to the relativistic motor effect; see Figure 8.

One can see that the positive relativistic motor effect near the proton at a distance r_{min} is much greater than the negative relativistic motor effect that occurs due to the motion in the opposite direction but at a much larger separation r_{max}. We also notice that the orthogonal motions will cancel each other as they occur in opposite directions. Unfortunately, such a description is not very useful as quantum effects play a major role in confined electron; thus, we conclude our discussion regarding classical electrons and move to the discussion of quantum electrons.

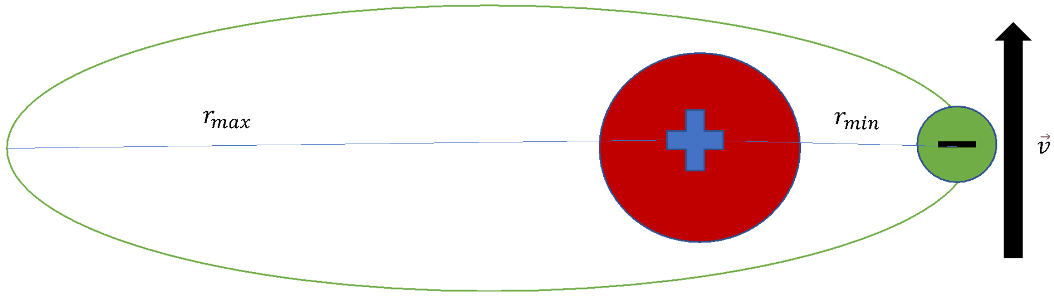

Figure 8. A schematic of an elliptical orbit of an electron around a proton.

3. Schrödinger's Electron

Quantum mechanics according to the Copenhagen interpretation has lost faith in our ability to predict precisely the whereabouts of even a single particle. However, the theory does predict precisely the evolution in time of the quantum wave function, which is related to a particle location in a probabilistic way. This evolution is described by Schrödinger's equation [17]:

$$i\hbar\dot{\psi} = \hat{H}_S\psi, \qquad \hat{H}_S = -\frac{1}{2m_e}\left(\hbar\vec{\nabla} - ie\vec{A}\right)^2 - e\Phi \tag{30}$$

where $i \equiv \sqrt{-1}$ and ψ is a complex function. $\dot{\psi} \equiv \frac{\partial\psi}{\partial t}$. $\hbar = \frac{h}{2\pi}$ is Planck's constant over 2π. However, this form of quantum theory is abstract and does not explicitly give a physical picture of the relevant quantities. Thus, we write the quantum function using the modulus a and phase ϕ representation:

$$\psi = ae^{i\phi}. \tag{31}$$

The probability density and flux are defined as

$$\tilde{\rho} = \psi^*\psi, \qquad \vec{J}_S = \frac{\hbar}{2m_e i}[\psi^*\vec{\nabla}\psi - (\vec{\nabla}\psi^*)\psi] - \frac{e}{m_e}\vec{A}\tilde{\rho} = \tilde{\rho}(\frac{\hbar}{m_e}\vec{\nabla}\phi - \frac{e}{m_e}\vec{A}). \tag{32}$$

We thus define the velocity field using the natural definition:

$$\vec{v}_S = \frac{\vec{J}_S}{\tilde{\rho}} = \frac{\hbar}{m_e}\vec{\nabla}\phi - \frac{e}{m_e}\vec{A} \tag{33}$$

and the mass density is

$$\hat{\rho} = m_e\tilde{\rho} = m_e a^2. \tag{34}$$

It follows from Equation (30) that the continuity equation is satisfied:

$$\frac{\partial\hat{\rho}}{\partial t} + \vec{\nabla}\cdot(\hat{\rho}\vec{v}_S) = 0 \tag{35}$$

Thus, $\vec{v}_S$ is the velocity associated with continuity. However, it is also the velocity field associated with the probability a^2 (by Born's interpretational postulate) and the charge density $\rho = ea^2$. The equation for the phase ϕ derived from Equation (30) takes the form

$$\hbar\frac{\partial\phi}{\partial t} + \frac{1}{2m_e}\left(\hbar\vec{\nabla}\phi - e\vec{A}\right)^2 - e\Phi = \frac{\hbar^2\nabla^2 a}{2m_e a} = -Q \tag{36}$$

In terms of the velocity defined in Equation (33), the following equation of motion [18,19] is obtained:

$$\frac{d\vec{v}_S}{dt} = \frac{\partial\vec{v}_S}{\partial t} + (\vec{v}_S\cdot\vec{\nabla})\vec{v}_S = -\vec{\nabla}\frac{Q}{m_e} + \frac{e}{m_e}(\vec{E} + \vec{v}\times\vec{B}) \tag{37}$$

The "quantum correction" for the classical equation can be found on the right-hand side of the above equation:

$$Q = -\frac{\hbar^2}{2m_e}\frac{\vec{\nabla}^2\sqrt{\hat{\rho}}}{\sqrt{\hat{\rho}}}. \tag{38}$$

The correction can be interpreted in terms of information theory [20,21]. These results illustrate the advantages of using phase and modulus variables to obtain classically looking equations of motion that have a substantially different form than the Schrödinger equation (but having the same mathematical content) and have obvious interpretation [22].

The quantum correction Q will disappear in the limit $\hbar \to 0$, but even if one intends to consider the quantum equation fully, one is forced to consider the expansion of an unconfined quantum function. Since Q is related to the gradient of the amplitude, it is obvious that as the function becomes smeared over time and the gradient becomes small, the quantum correction becomes negligible. To put it in quantitative terms,

$$\vec{F}_Q = -\vec{\nabla}Q \simeq \frac{\hbar^2}{2m_e L_R^3}, \qquad L_R \simeq \frac{R}{|\vec{\nabla}R|} \tag{39}$$

L_R is the length of the amplitude gradient. Thus,

$$|F_Q| << |F_L| \Rightarrow L_R >> L_{Rc} = \left(\frac{\hbar^2}{2m_e F_L}\right)^{\frac{1}{3}}. \tag{40}$$

in which $\vec{F}_L = e(\vec{E} + \vec{v} \times \vec{B})$ is the Lorentz force [23,24]. For the free electron relativistic motor in which an electron transverses a macroscopic length, this term will be negligible. However, for a confined electron, this term should not be neglected as we show in the section describing the hydrogen atom.

4. Pauli's Electron

Schrödinger's mechanics describes spinless particles. The need for spin became necessary for describing the Stern–Gerlach experiments, as Schrödinger predicted a single spot instead of the two spots obtained for hydrogen atoms. Thus, Pauli suggested a nonrelativistic particle with the spin equation

$$i\hbar\dot{\psi} = \hat{H}_P\psi, \qquad \hat{H}_P = -\frac{\hbar^2}{2m_e}[\vec{\nabla} - \frac{ie}{\hbar}\vec{A}]^2 + \mu\vec{B}\cdot\vec{\sigma} + e\Phi = \hat{H}_S\, I + \mu\vec{B}\cdot\vec{\sigma} \tag{41}$$

In the above equation, ψ is a complex column vector of two dimensions (a spinor), $\hat{H}_P$ is a Hermitian operator matrix, μ is the magnetic moment of the particle, and I is a unit matrix. $\vec{\sigma}$ is a vector of Pauli matrices:

$$\sigma_1 = \begin{pmatrix} 0 & 1 \\ 1 & 0 \end{pmatrix}, \qquad \sigma_2 = \begin{pmatrix} 0 & -i \\ i & 0 \end{pmatrix}, \qquad \sigma_3 = \begin{pmatrix} 1 & 0 \\ 0 & -1 \end{pmatrix}. \tag{42}$$

The ad hoc status of this equation was later removed as it was shown to be the nonrelativistic limit of the relativistic Dirac equation. If ψ satisfies Equation (41), it must also satisfy

$$\frac{\partial\rho_P}{\partial t} + \vec{\nabla}\cdot\vec{j} = 0, \tag{43}$$

in which

$$\rho_P = \psi^\dagger\psi, \qquad \vec{j} = \frac{\hbar}{2m_e i}[\psi^\dagger\vec{\nabla}\psi - (\vec{\nabla}\psi^\dagger)\psi] - \frac{e}{m_e}\vec{A}\rho_P. \tag{44}$$

$\psi^\dagger$ is a row spinor (the transpose) whose components are equal to the complex conjugate of ψ. Equation (43) suggests a velocity field as follows [19]:

$$\vec{v} = \frac{\vec{j}}{\rho_p} = \frac{\hbar}{2m_e i \rho_p}[\psi^\dagger \vec{\nabla}\psi - (\vec{\nabla}\psi^\dagger)\psi] - \frac{e}{m_e}\vec{A}. \tag{45}$$

Holland [19] suggested to write the spinor in the following form:

$$\psi = Re^{i\frac{\chi}{2}} \begin{pmatrix} \cos\left(\frac{\theta}{2}\right)e^{i\frac{\phi}{2}} \\ i\sin\left(\frac{\theta}{2}\right)e^{-i\frac{\phi}{2}} \end{pmatrix} \equiv \begin{pmatrix} \psi_\uparrow \\ \psi_\downarrow \end{pmatrix}. \tag{46}$$

Thus the probability density is given as

$$R^2 = \psi^\dagger \psi = \rho_p \Rightarrow R = \sqrt{\rho_p}. \tag{47}$$

The mass density is given by

$$\hat{\rho} = m_e \psi^\dagger \psi = m_e R^2 = m_e \rho_p. \tag{48}$$

Additionally, we obtain probability amplitudes for spin-up and spin-down electrons:

$$a_\uparrow = |\psi_\uparrow| = R\left|\cos\frac{\theta}{2}\right|, \qquad a_\downarrow = |\psi_\downarrow| = R\left|\sin\frac{\theta}{2}\right|. \tag{49}$$

The other Holland variables can be interpreted in terms of the expectation value of the spin in the following way:

$$< \frac{\hbar}{2}\vec{\sigma} >= \frac{\hbar}{2}\int \psi^\dagger \vec{\sigma}\psi d^3x = \frac{\hbar}{2}\int \left(\frac{\psi^\dagger \vec{\sigma}\psi}{\rho_p}\right)\rho_p d^3x \tag{50}$$

The spin density is

$$\hat{s} \equiv \frac{\psi^\dagger \vec{\sigma}\psi}{\rho_p} = (\sin\theta\sin\phi, \sin\theta\cos\phi, \cos\theta), \qquad |\hat{s}| = \sqrt{\hat{s}\cdot\hat{s}} = 1. \tag{51}$$

Thus, θ, ϕ are angles of the projection of the spin density on the axes. θ is an elevation angle, and ϕ is an the azimuthal angle. The velocity field can be presented by Holland's variables by using both Equations (45) and (46):

$$\vec{v} = \frac{\hbar}{2m_e}(\vec{\nabla}\chi + \cos\theta\vec{\nabla}\phi) - \frac{e}{m_e}\vec{A}. \tag{52}$$

The material derivative of the velocity is thus ([19], p. 393, Equation (9.3.19))

$$\frac{d\vec{v}}{dt} = -\vec{\nabla}(\frac{Q}{m_e}) - \left(\frac{\hbar}{2m_e}\right)^2 \frac{1}{\rho_p}\partial_k(\rho_p \vec{\nabla}\hat{s}_j \partial_k \hat{s}_j) + \frac{e}{m_e}(\vec{E} + \vec{v}\times\vec{B}) - \frac{\mu}{m_e}(\vec{\nabla}B_j)\hat{s}_j. \tag{53}$$

Pauli's equation of motion differs from both the classical equation and Schrödinger's equation. In addition to the Schrödinger quantum force, we have an additional spin quantum force:

$$\vec{F}_{QS} \equiv -\frac{\hbar^2}{4m_e}\frac{1}{\rho_p}\partial_k(\rho_p \vec{\nabla}\hat{s}_j \partial_k \hat{s}_j) = -\frac{\hbar^2}{4m_e}\left[\partial_k(\vec{\nabla}\hat{s}_j \partial_k \hat{s}_j) + \frac{\partial_k \rho_p}{\rho_p}\vec{\nabla}\hat{s}_j \partial_k \hat{s}_j\right] \tag{54}$$

Additionally, we have a Stern–Gerlach term describing the interaction of the spin with a gradient of the magnetic field:

$$\vec{F}_{gradBS} \equiv -\mu(\vec{\nabla}B_j)s_j. \tag{55}$$

Since the upper and lower spin components are expanding in free space, it follows that the gradients of $\vec{F}_{QS}$ will tend to diminish for any macroscopic scale, making this force negligible. To estimate the condition, we introduce the typical spin length:

$$L_s = \min{}_{i\in\{1,2,3\}} |\vec{\nabla}\hat{s}_i|^{-1} \tag{56}$$

Using the above definition, we may estimate the spin quantum force:

$$F_{QS} \approx \frac{\hbar^2}{4m}[\frac{1}{L_s^3} + \frac{1}{L_s^2 L_R}] = \frac{\hbar^2}{4mL_s^2}[\frac{1}{L_s} + \frac{1}{L_R}] \tag{57}$$

This suggests a hybrid typical length:

$$L_{sR} = [\frac{1}{L_s} + \frac{1}{L_R}]^{-1} = \begin{cases} L_s & L_s \ll L_R \\ L_R & L_R \ll L_s \end{cases}, \tag{58}$$

in terms of which

$$F_{QS} \approx \frac{\hbar^2}{4m_e L_s^2 L_{sR}} \tag{59}$$

Thus,

$$F_{QS} \ll F_L \Rightarrow L_s^2 L_{sR} \gg \frac{\hbar^2}{4m_e F_L} \Rightarrow L_s \gg \begin{cases} \left(\frac{\hbar^2}{4m_e F_L}\right)^{\frac{1}{3}} & L_s \ll L_R \\ \left(\frac{\hbar^2}{4m_e F_L L_R}\right)^{\frac{1}{2}} & L_R \ll L_s \end{cases}. \tag{60}$$

In the free electron scenario, the only quantum term that might have a significance is the Stern–Gerlach term given in Equation (55); however, it is well known that this term is negligible with respect to the Lorentz classical term, which is why Stern–Gerlach experiments are performed using natural particles. Thus, as far as free-electrons-based relativistic engines are concerned, a classical analysis will suffice; this is not the case for a confined electron, as we discuss in the next section.

5. The Hydrogen Atom

The hydrogen atom is a simple quantum system and was discussed in [4,25]; we will use the same notation as in [4] and will not redefine the notation here.

The associated velocity field of an eigenfunction is determined from its phase (Equation (44) in [4]), which is

$$\vec{v}_S = \frac{\hbar}{m_e}\vec{\nabla}\phi - \frac{e}{m_e}\vec{A} = \frac{m\hbar}{m_e r \sin\theta'}\hat{\varphi}, \qquad \vec{A} = 0, \tag{61}$$

and is azimuthal; thus, for every eigenstate, the electron is circulating some axis (the z axis, which is arbitrarily defined). The speed of the electron in the hydrogen atom is thus

$$v_S = \frac{m\hbar}{m_e r |\sin\theta'|}. \tag{62}$$

The speed will vanish for every eigenstate with a magnetic quantum number $m = 0$, including for the ground state. However, for every other magnetic quantum number, the velocity field is singular both in the proton at $r = 0$ and on the north and south poles $\theta' = 0, \pi$. Regrading the singularity at $r = 0$, this is not a problem from a physical point of view as one can expect a different potential from the Coulomb potential inside the proton, which is not a point particle. However, with regard to the south and north poles' infinite velocities, this indicates a difficulty in the hydrogen atom classical description in which relativistic considerations that enforce speeds smaller than the velocity of light c will be part of the solution. The static electron implies, according to Equation (37), that the force is zero. This is indeed the case. One can calculate the quantum potential for every state by using Equation (38); however, for hydrogen eigenstates, it will be easier to use Equation (36) and substitute the phase from Equation (44) of [4]. This gives the expression

$$Q_{nm} = E_n - \frac{m^2\hbar^2}{2m_e r^2 \sin^2\theta'} + e\Phi = E_n - \frac{m^2\hbar^2}{2m_e r^2 \sin^2\theta'} + \frac{ke^2}{r} \tag{63}$$

This can be verified by the direct substitution of eigenstates in Equation (38). It is easy to see that for $m = 0$, the total force vanishes:

$$\vec{\nabla}(Q_{nm} - e\Phi) = \vec{\nabla}E_n = 0 \tag{64}$$

Thus, the current density of Equation (32) is

$$\vec{J} = \frac{\hbar}{m_e}\rho\vec{\nabla}\phi = -m\frac{e\hbar}{m_e}|\psi_{nlm}|^2\frac{\hat{\varphi}}{r\sin\theta'} \tag{65}$$

The current density is linear in the magnetic number m; if $m = 0$, the current density is null and there is no relativistic motor force. It follows that for an isolated hydrogen in the ground state $n = 1, l = 0, m = 0$, there is no relativistic motor force. In excited states for which the current density is not null, there will be no relativistic motor force if the potential is spherically symmetric as is evident from Equation (3) of [4].

It seems that a hydrogen atom cannot be used in a relativistic motor. However, this system can be manipulated by chemical and electromagnetic means, as described in [4]. To understand the order of magnitude of the relativistic motor effect using a hydrogen atom, one is referred to [4].

6. A Simple Wave Packet

We consider an idealized wave packet:

$$\psi = Ae^{ik'x}, \qquad A = \begin{cases} \sqrt{\tilde{\rho}_c} & r < R_{max} \\ 0 & r \geq R_{max} \end{cases} \tag{66}$$

k' and $\tilde{\rho}_c$ are constants. Since the wave function is normalized, it follows that

$$\tilde{\rho}_c = \frac{3}{4\pi}R_{max}^{-3} \tag{67}$$

The phase of this wave function is linear, and its amplitude is uniform inside a sphere of radius R_{max}. It is not an eigenstate of the hydrogen atom Hamiltonian; the preparation of such a state will require a suitable electromagnetic field, which will be discussed below. We have analyzed the properties of this wave function in [4] and will not repeat the analysis here.

The purpose of wave function engineering is to achieve a wave function that will produce a stable linear momentum over macroscopic durations. This implies, according to Equation (3) of [4] and Equation (32), that we need to achieve a constant wave packet amplitude and constant phase gradient affected by a constant vector potential. A constant phase gradient does not imply a constant phase; in fact, we may write the phase in the form

$$\phi = \phi_s(\vec{x}) - \phi_t(t) \tag{68}$$

For a time-independent amplitude, it follows from Equation (31) that

$$\frac{\partial\psi}{\partial t} = -i\psi\frac{\partial\phi_t}{\partial t} \tag{69}$$

defining

$$E(t) = \hbar \frac{\partial \phi_t}{\partial t} \tag{70}$$

which is a time-dependent function with units of energy; Schrödinger Equation (30) implies that

$$\hat{H}_S \psi = E(t)\psi \tag{71}$$

Thus, to achieve such a condition, ψ must be an eigenfunction of some Hamiltonian $\hat{H}_S$ with a possibly time-dependent eigenvalue $E(t)$. A Hamiltonian can be constructed by introducing suitable electromagnetic fields into the physical system. For example, let us consider the somewhat artificial wave packet described in Equation (66), which we now augment with a time-dependent phase:

$$\psi = Ame^{i(k'x - \phi_t(t))}, \qquad Am = \begin{cases} \sqrt{\tilde{\rho}_c} & r < R_{max} \\ 0 & r \geq R_{max} \end{cases} \tag{72}$$

We shall now plug the above expression into Equation (30) and ignore the nonphysical derivatives connected to the fact that the above oversimplified wave packet is not smooth at $r = R_{max}$; it follows that

$$E(t) = \frac{\hbar^2 k'^2}{2m_e} - e\Phi - \frac{e\hbar k'}{m_e} A_x + \frac{e^2 A^2}{2m_e}, \tag{73}$$

Above, we took advantage of the gauge freedom and assumed a Coulomb gauge $\vec{\nabla} \cdot \vec{A} = 0$, which is of course not physically restrictive. This allows two types of solutions. In one case, we assume $A_x = 0$; that is, we assume that there is no vector potential component in the direction of motion of the wave packet. Denoting the perpendicular vector potential as $\vec{A}_\perp = A_y \hat{y} + A_z \hat{z}$, it follows that

$$A_\perp = \pm \frac{\sqrt{2m_e}}{e} \sqrt{E(t) + e\Phi - \frac{\hbar^2 k'^2}{2m_e}}. \tag{74}$$

If, however, $A_x \neq 0$, it follows that

$$A_x = \frac{1}{e} \left(\hbar k \pm \sqrt{2m_e E(t) - e^2 A_\perp^2 + 2m_e e\Phi} \right). \tag{75}$$

7. Discussion

The main results of this paper are the implementation of a relativistic motor on the atomic scale. It is demonstrated that two approaches are possible. In one case, we consider free propagating electrons, which move, nevertheless, in proximity to the nucleus but have enough energy not to be captured by the nucleus; we also consider the case of confined electrons.

Free electrons are classical, and quantum forces are shown to be negligible due to the phenomenon of wave packet spreading; thus, a relativistic engine based on free electrons is analyzed classically.

For confined electrons, quantum effects are important. Unfortunately, an isolated hydrogen atom in either a ground or excited state does not produce relativistic motor momentum. We study the case in which an electron is put in a wave packet state that is an eigenstate of an unspecified Hamiltonian. The electromagnetic field for generating such a Hamiltonian is calculated.

8. Conclusions

Despite the theoretical possibility of constructing a working relativistic motor, in practice, this will not be a trivial task and will involve the generation of a highly localized wave packet or, alternatively, a very narrow electron beam. This is so because an **isolated** hydrogen atom in either a ground or excited state does not produce relativistic motor momentum.

Thus, in a study that is not merely preliminary as this one, a more realistic wave packet should be considered, and the sources of the electromagnetic field needed to achieve this goal need to be specified. Alternatively, one will need to describe how to accelerate a very narrow beam of electron that will fit within a lattice constant.

Additional suggestions for studies that may follow this paper include the following:

1. Analysis of a relativistic engine with components that move at relativistic speeds (and not just the electromagnetic signals transmitted between the components). The need for this arises as the electron studied in the current paper is relativistic.
2. A study of the relativistic motor in the framework of a Dirac theory is required. The Schrödinger equation and the Pauli equation are not sufficient for the study of an electron at relativistic speeds.

Funding: This research received no external funding.

Data Availability Statement: Data sharing not applicable.

Conflicts of Interest: The author declares no conflict of interest.

References

1. Tuval, M.; Yahalom, A. Momentum Conservation in a Relativistic Engine. *Eur. Phys. J. Plus* **2016**, *131*, 374. [CrossRef]
2. Feynman, R.P.; Leighton, R.B.; Sands, M.L. *Feynman Lectures on Physics*, 50th ed.; Basic Books: New York, NY, USA, 2011.
3. Jackson J.D. *Classical Electrodynamics*, 3rd ed.; Wiley: New York, NY, USA, 1999.
4. Yahalom, A. Newton's Third Law in the Framework of Special Relativity for Charged Bodies Part 2: Preliminary Analysis of a Nano Relativistic Motor. *Symmetry* **2022**, *14*, 94. [CrossRef]
5. Tuval, M.; Yahalom, A. Newton's Third Law in the Framework of Special Relativity. *Eur. Phys. J. Plus* **2014**, *129*, 240. [CrossRef]
6. Griffiths, D.J.; Heald, M.A. Time dependent generalizations of the Biot-Savart and Coulomb laws. *Am. J. Phys.* **1991**, *59*, 111–117. [CrossRef]
7. Jefimenko, O.D. *Electricity and Magnetism*, 2nd ed.; Electret Scientific: Star City, WV, USA, 1989.
8. Yahalom, A. Retardation in Special Relativity and the Design of a Relativistic Motor. *Acta Phys. Pol. A Vol.* **2017**, *131*, 1285–1288. [CrossRef]
9. Mansuripur, M. Trouble with the Lorentz Law of Force: Incompatibility with Special Relativity and Momentum Conservation. *PRL* **2012**, *108*, 193901. [CrossRef] [PubMed]
10. Rajput, S.; Yahalom, A.; Qin, H. Lorentz Symmetry Group, Retardation and Energy Transformations in a Relativistic Engine. *Symmetry* **2021**, *13*, 420. [CrossRef]
11. Shailendra, R.; Yahalom, A. Newton's Third Law in the Framework of Special Relativity for Charged Bodies. *Symmetry* **2021**, *13*, 1250. [CrossRef]
12. Dielectric Strength of Air—The Physics Fact Book. Available online: https://hypertextbook.com/facts/2000/AliceHong.shtml (accessed on 20 August 2023).
13. Giere, S.; Kurrat, M.; Schumann, U. HV Dielectric Strength of Shielding Electrodes in Vacuum Circuit-Breakers. In Proceedings of the 20th International Symposium on Discharges and Electrical Insulation in Vacuum, Tours, France, 1–5 July 2002.
14. Volpe, P.-N.; Muret, P.; Pernot, J.; Omnès, F.; Teraji, T.; Jomard, F.; Planson, D.; Brosselard, P.; Dheilly, N.; Vergne, B.; Scharnholtz, S. High breakdown voltage Schottky diodes synthesized on p-type CVD diamond layer. *Phys. Status Solidi A* **2010**, *207*, 2088–2092. Available online: https://onlinelibrary.wiley.com/doi/abs/10.1002/pssa.201000055 (accessed on 10 August 2013). [CrossRef]
15. Lo, H.W.; Tai, Y.C. Parylene-based electret power generators. *J. Micromech. Microeng.* **2008**, *18*, 104006. [CrossRef]
16. Jung, S.-G.; Kang, J.-H.; Park, E.; Lee, S.; Lin, J.-Y.; Chareev, D.A.; Vasiliev, A.N.; Park, T. Enhanced critical current density in the pressure-induced magnetic state of the high-temperature superconductor FeSe. *Sci. Rep.* **2015**, *5*, 16385. [CrossRef] [PubMed]
17. Schrödinger, E. *Collected Papers in Wave Mechanics*; Blackie and Sons: London, UK, 1928; p. 102.
18. Madelung, E. Quantum Theory in Hydrodynamical Form. *Z. f. Phys.* **1927**, *40*, 322.
19. Holland, P.R. *The Quantum Theory of Motion*; Cambridge University Press: Cambridge, UK, 1993.
20. Yahalom, A. The Fluid Dynamics of Spin. *Mol. Phys.* **2018**, *116*, 1–11. [CrossRef]
21. Yahalom, A. The Fluid Dynamics of Spin—A Fisher Information Perspective and Comoving Scalars. *Chaotic Model. Simul. (CMSIM)* **2020**, *1*, 17–30.
22. Bohm, D. *Quantum Theory*; Prentice Hall: New York, NY, USA, 1966 .
23. Yahalom, A. Pauli's Electron in Ehrenfest and Bohm Theories, a Comparative Study. *Entropy* **2023**, *25*, 190. [CrossRef] [PubMed]

24. Yahalom, A. Fisher Information Perspective of Pauli's Electron. *Entropy* **2022**, *24*, 1721. [CrossRef] [PubMed]
25. Humphreys, C.J. The Sixth Series in the Spectrum of Atomic Hydrogen. *J. Res. Natl. Bur. Stand.* **1953**, *50*, 432. [CrossRef]